

Temporal Profiling of the Coding and Noncoding Murine Cytomegalovirus Transcriptomes^{▼†}

Paul Lacaze,^{1,*} Thorsten Forster,¹ Alan Ross,¹ Lorraine E. Kerr,² Eliane Salvo-Chirnside,² Vanda Juranic Lisnic,³ Guillermo H. López-Campos,⁴ José J. García-Ramírez,⁵ Martin Messerle,⁶ Joanne Trgovcich,⁷ Ana Angulo,⁸ and Peter Ghazal^{1,2*}

Division of Pathway Medicine, The University of Edinburgh, The Chancellor's Building, College of Medicine, 49 Little France Crescent, Edinburgh, United Kingdom¹; Centre for Systems Biology at Edinburgh, The University of Edinburgh, Darwin Building, King's Buildings Campus, Mayfield Road, Edinburgh, United Kingdom²; Department of Histology and Embryology, Faculty of Medicine, Rijeka University, Croatia³; Área de Bioinformática y Salud Pública, Instituto de Salud Carlos III, 28220 Madrid, Spain⁴; Department of Inorganic and Organic Chemistry and Biochemistry, Medical School, Regional Center for Biomedical Research, University of Castilla-La Mancha, Avenida de Almansa 14, 02006 Albacete, Spain⁵; Department of Virology, Hannover Medical School, Hannover, Germany⁶; Department of Pathology, The Ohio State University, Columbus, Ohio 43210⁷; and Institut d'Investigacions Biomèdiques August Pi i Sunyer (IDIBAPS), Barcelona, Spain⁸

Received 9 November 2010/Accepted 28 March 2011

The global transcriptional program of murine cytomegalovirus (MCMV), involving coding, noncoding, and antisense transcription, remains unknown. Here we report an oligonucleotide custom microarray platform capable of measuring both coding and noncoding transcription on a genome-wide scale. By profiling MCMV wild-type and immediate-early mutant strains in fibroblasts, we found rapid activation of the transcriptome by 6.5 h postinfection, with absolute dependency on *ie3*, but not *ie1* or *ie2*, for genomic programming of viral gene expression. Evidence is also presented to show, for the first time, genome-wide noncoding and bidirectional transcription at late stages of MCMV infection.

Murine cytomegalovirus (MCMV) is a ubiquitous betaherpesvirus with a 235-kbp genome transcribed in a classical cascade fashion (55). The genome sequence of MCMV has been available for some time (89), and yet a systematic study of temporal gene expression during MCMV infection has been lacking. Double-stranded PCR-based cDNA microarrays were used once previously (105) to validate the expression of a subset of predicted MCMV open reading frames (ORFs) (15) at a single time point (24 h postinfection [hpi]). More-advanced microarray technology based on oligonucleotide probes, affording increased specificity to distinguish RNA polarity, has not been reported. For human cytomegalovirus (HCMV), abundant antisense (AS) transcription has been observed (120), raising the possibility that aspects of the CMV life cycle are influenced or regulated by noncoding transcripts. For MCMV, small virus-encoded microRNAs (miRNAs) (19, 20, 33) and larger double-stranded RNAs (21, 110) have been reported to be transcribed from multiple loci; however, the frequency and abundance of noncoding transcripts throughout the MCMV genome have not yet been measured systematically on a genome-wide scale and at multiple stages of infection.

Here we have investigated the global transcriptional program of MCMV by constructing a microarray capable of mea-

suring sense (S) and AS transcripts. Microarrays were designed using 55-mer oligonucleotide probes in sense and antisense orientations to each of the 170 viral ORFs predicted in the MCMV genome (89). One hundred ninety-two positive-control probes were designed against stably expressed mouse genes for normalization purposes, and 97 negative-control probes were designed against *Saccharomyces cerevisiae* sequences with no homology to mouse or MCMV genomes (for probe sequences, see Table S1 in the supplemental material). The 55-mer oligonucleotide probes were diluted to a concentration of 60 μM and inkjet printed (Arrayjet, United Kingdom) onto amino silane-coated glass slides, with each microarray consisting of six identical subarrays. Probes were printed in triplicate per array and have the capacity for developing a total of 18 measurements per probe per sample to ensure high technical replication. Target RNA was extracted from infected fibroblasts using PureLink RNA minikits with on-column DNase I treatment (Invitrogen, CA). Purified RNA (700 ng for each sample) was labeled for microarray analysis using the Agilent low-input fluorescent linear amplification protocol (Agilent, CA), with 3 μg of Cy5-labeled target cRNA hybridized per sample. Hybridized microarrays were washed and subsequently scanned using an Agilent (CA) G2505B scanner.

To perform a systematic analysis of genome-wide transcription in MCMV, we infected NIH 3T3 fibroblasts with the parental MCMV strain at a multiplicity of infection (MOI) of 1 and performed DNA microarray analysis on total RNA harvested from duplicate cultures at 0.5, 6.5, 24, and 48 hpi. Individual probe signals were background subtracted, median summarized, and log base 2 transformed to form raw data points (see Table S2 in the supplemental material). Raw data were quality controlled, and normalization between samples

* Corresponding author. Mailing address: Division of Pathway Medicine, University of Edinburgh Medical School, The Chancellor's Building, 49 Little France Crescent, Edinburgh EH16 4SB, United Kingdom. Phone: 44 131 242 6284. Fax: 44 131 242 6244. E-mail for P. Ghazal: p.ghazal@ed.ac.uk. E-mail for P. Lacaze: paul.lacaze@ed.ac.uk.

† Supplemental material for this article may be found at <http://jvi.asm.org/>.

[▼] Published ahead of print on 6 April 2011.

TABLE 1. High-confidence MCMV microarray sense probes^a

Unique probe ID ^b	ORF	Strand	MCMV name	HCMV name	Time on ^c (hp)	Protein type	Annotation ^d (reference[s])	Virion association ^e
vMC132	m128 Ex3	C	ie2	US22 (GF2)	0.5	Immediate early	Spliced m128 (ie2) gene has sequence similarity to members of the US22 family of HCMV (77)	
vIE1rem	m123 Ex4	C	ie1	IE1	6.5	Immediate early	ie1 exon 4, with mRNA terminating at base 179544 (53–55); total length of Ex2 plus Ex3 plus Ex4 is 595 aa, total molecular size is 66.7 kDa	
vMC003	m03				6.5	Glycoprotein m02	Sequence variation and early transcriptional kinetics found in wild-type-derived MCMV isolates; m03-encoded protein could be found on cell surface (28)	
vMC004	m04		gp34		6.5	Glycoprotein m02	m04 gene product (gp34) forms a complex with MHC-I (51), which reaches the cell surface (46) and is required for Ly49P recognition of infected cells (57); m04/gp34 also antagonizes the effect of m152 (84)	
vMC006	m06		gp48		6.5	Glycoprotein m02	m06 gene product (gp48) downmodulates the levels of MHC-I proteins in infected cells (50) and binds to the ternary complex of assembled MHC-I with antigenic peptide in the ER, redirecting this complex to the proteasome for degradation; unbound gp48 is destroyed by the proteasome (18)	
vMC008	m08				6.5	Glycoprotein m02	Glycoprotein family m02	
vMC010	m10				6.5	Glycoprotein m02	Glycoprotein family m02	
vMC016	m16.2				6.5	Glycoprotein m02	Glycoprotein family m02, probe overlaps with newly predicted ORF m16.2 (105)	VAP
vMC017	m17	C			6.5	Membrane glycoprotein		
vMC018	m18	C			6.5	Early US22 family homolog		
vMC027	m25.1	C		UL23 (GF2)	6.5			
vMC030	M28	C		UL28	6.5			
vMC037	m34.2			UL34	6.5			
vMC040	M36 Ex2	C		UL36 exon 2	6.5	US22 family homolog	Reannotations of the MCMV genome have identified three putative M34-overlapping ORFs (m33.1, m34.1, and m34.2); this microarray probe overlaps with newly predicted ORF m34.2 (105); an M34 mutant virus which interrupted all three m34 ORFs had attenuated replication both in tissue culture and in SCID mice (10)	
vMC041	M37	C		UL37	6.5	Glycoprotein	Possible transcriptional regulator (89), implicated in blocking apoptosis via inhibition of caspase-8 (FLICE) activation (100); growth of M36 mutant was attenuated <i>in vitro</i> and <i>in vivo</i> (27); HCMV vICApUL26 protects cells from extrinsic apoptosis induced via death receptors in TNFR1, Fas/CD95, or Trail Glycoprotein, vMIA; M37 mutant is severely attenuated in growth and virulence <i>in vivo</i> (63); homolog of HCMV UL37 that inhibits mitochondrial megapore activation in a manner similar to members of the antiapoptotic Bcl family (37); may also be a transcriptional regulator (88)	
vMC045	m41	C			6.5	Putative glycoprotein	Putative antiapoptotic function (79)	
vMC046	m42	C			6.5	US22 family homolog		
vMC047	M43	C		UL43	6.5			
vMC049	M45	C		UL45 (RRL)	6.5	Ribonucleotide reductase	Antiapoptotic (79), immunoregulatory gene that modulates T helper cell response (99); found to be nonessential for viral growth <i>in vitro</i> and <i>in vivo</i> and dispensable for virulence in killing SCID mice (117)	VAP
vMC055	m48.2	C			6.5	Capsid	Antiapoptotic (17) homologue of the large subunit of ribonucleotide reductase (85); blocks NF- <kappa>B activation as a result of its inhibitory effect on RIP1 signaling (71, 109)</kappa>	VAP
vMC061	M54	C	DNApol	UL54 (DNapol)	6.5	DNA polymerase delta subunit (59)	Smallest capsid protein (14)	VAP
vMC064	M57	C		UL57 (MDBP)	6.5	Major ssDNA binding protein (3, 4)	Major ssDNA binding protein (3, 4)	VAP
vMC079	M80	C		UL80 (AP)	6.5	Assembly protein and protease (11, 69) that conserves the domain structure and cleavage sites present in HCMV UL80	Assembly protein and protease (11, 69) that conserves the domain structure and cleavage sites present in HCMV UL80	VAP
vMC080	M82	C	pp71	UL82 (pp71)	6.5	Upper matrix phosphoprotein	Encodes a structural protein unique to the betaherpesvirus group, also known as pp71; same family as M83 (91)	VAP
vMC092	M94	C		UL94	6.5	Virion-associated phosphoprotein	Virion-associated, tegument/second envelopment protein (112)	VAP
vMC098	M99			UL99 (pp28)	6.5	Phosphoprotein	Encodes small structural phosphoprotein unique to the betaherpesvirus group, shown to be around 16 kDa in size and to be associated with the virion (30, 78)	VAP
vMC100	M102			UL102 (HP)	6.5	Helicase-prime	Part of the helicase-prime complex of three proteins (M70, M102, and M105) (70, 97)	VAP
vMC103	M105			UL105 (Hel)	6.5	DNA helicase	DNA helicase; part of the helicase-prime complex of three proteins (M70, M102, and M105) (70, 97)	VAP
vMC114	M118	C		UL118	6.5		Possible alternate splice to m119, as for HCMV UL118 (62, 88)	
vMC117	m119.2	C	sgg1		6.5		Exon 2 of M133 (sgg1) (61, 73)	
vMC136	m132 Ex2	C			6.5			

vMC141	m137	C	Fegr	fcr1	6.5	Putative glycoprotein	
vMC142	m138	C			6.5	Glycoprotein	
vMC146	m142	C		US26 (GF2)	6.5	US22 family homolog	
vMC151	m147	C			6.5	Possible membrane-spanning protein	
vMC156	m152	C	gp40		6.5	Glycoprotein	
vMC158	m154	C			6.5	Glycoprotein	
vMC164	m160	C			6.5	Putative membrane glycoprotein	
vMC167	m163	C			6.5	Putative membrane glycoprotein	
vMC168	m164	C	gp36.5		6.5	Putative membrane glycoprotein	
vMC170	m166	C			6.5	Putative membrane glycoprotein	
vMC173	m169	C	ie3	UL122 (IE2)	6.5	Immediate early	
vME3rem	M122_Ex5	C			24		
vMC011	m11				24	Glycoprotein m02	
vMC013	m13				24	Glycoprotein m02	
vMC015	m15				24	Glycoprotein m02	
vMC020	m20	C			24		
vMC023	M23	C		UL23 (GF2) P	24		
vMC026	M25	C		UL25 (GFI)	24	Tegument	
vMC028	M26	C		UL26	24		
vMC029	M27	C		UL27	24		
vMC032	m29.1				24		
vMC033	m30				24		
vMC034	M31			UL31	24		
vMC035	M32	C		UL32 (pp150)	24	Phosphoprotein (tegument)	
vMC038	M35			UL35 (GFI)	24	Virion associated	
vMC039	M36_Ex1			UL36 exon 1	24		
vMC042	M38	C		UL38	24		
vMC050	m45.1	C		UL48 (Teg)	24	Tegument	
vMC053	M48			UL49	24		
vMC056	M49	C		UL50	24	Nuclear export	
vMC057	M50	C					
vMC059	M52			UL52	24		
vMC060	M53			UL53	24		
vMC062	M55	C	gB	UL55 (gB)	24	Glycoprotein	
vMC063	M56	C		UL56 (NM)	24	Tegument	

Continued on following page

TABLE 1—Continued

Unique probe ID ^b	ORF	Strand	MCMV name	HCMV name	Time on ^c (hpi)	Protein type	Annotation ^d (reference[s])	Virion association ^e
vMC067	M69	C	UL69	UL69	24	Tegument	Teagument protein similar to HCMV transactivator UL69 (113), which in HCMV induces a G _i block (42)	VAP
vMC071	M72	C	UL72 (dUTPase)	UL72 (dUTPase)	24	Putative dUTPase	Homology to HCMV UL72, a putative dUTPase enzyme required for nucleotide metabolism, replication, and/or repair (86)	VAP
vMC072 vMC077	M73 M78		UL73 UL78		24 24	G protein-coupled receptor	G protein-coupled receptor homologue, same family as M33 (38); has subcellular trafficking properties (96); M78 mutants exhibit reduced replication in cultured cells as well as severe attenuation in the infected host (83)	VAP
vMC078 vMC081	M79 M83	C	UL79 UL83 (pp65)		24 24	Virion associated	Homologue of HCMV virion-associated factor with IFN repressor function (pp65) (1, 16, 74); M83 mutant has attenuated viral growth and virulence in SCID mice (119)	VAP
vMC083 vMC084 vMC086 vMC091 vMC093	M85 M86 M88 M93 M89_Ex1	C	UL85 UL86 (MCP)		24 24 24 24 24	Capsid Capsid Virion associated	Homologue of HCMV minor capsid protein (9) Homologue of HCMV major capsid protein (25) Homologue of HCMV virion protein (9)	VAP VAP VAP
vMC094 vMC095 vMC096 vMC097	M95 M96 M97		UL95 UL96 UL97 (PK)		24 24 24	Phosphotransferase	Homologue of HCMV UL97 phosphotransferase gene, whose product phosphorylates ganciclovir in HCMV-infected cells (67, 102)	VAP
vMC098 vMC099	M98 M100	C	gM	UL98 (DNase) UL100 (gM)	24 24	Exonuclease Glycoprotein	Alkaline exonuclease (DNase) gene (89) Glycoprotein M with seven hydrophobic stretches that are potential membrane-spanning regions (66, 93)	VAP VAP
vMC101 vMC104 vMC105 vMC106 vMC107	M103 m106 m107 m108 M112_Ex1	C	gM	UL103	24			
vMC107			e1	UL112	24	Early	Exon 1 of e1 (22); total e1 length is 330 aa, molecular size is 36.4 kDa; IE3 and the early M112/113 gene products colocalize and coimmunoprecipitate (104); neuron-specific activation of the e1 promoter observed in transgenic mice (7)	
vMC109	M114	C		UL114 (UNG)	24	Glycosylase	Uracil DNA glycosylase enzyme homolog (114) found in herpesviruses, required for nucleotide metabolism, replication, and/or repair	
vMC110	M115	C	gL	UL115 (gL)	24	Glycoprotein	M115 (gL) (52) contains five potential glycosylation sites, has significant amino acid similarity to gL homologs in HCMV and HHV-6, and has previously been shown to be glycosylated in virions (118)	
vMC115 vMC116 vMC119	m119 m119,1 m119,4 m119,5				24	Potential glycoprotein	Predicted MCMV homologue of HCMV spliced ORF (89)	
vMC120 vMC121 vMC123	m120 m121 M122_Ex5	C		UL122 (IE2)	24		ie3 exon 5, with mRNA terminating at base 177817 (76); total length of Ex2 plus Ex3 plus Ex5 is 611 aa, molecular size is 68.1 kDa	
vMC127	m124				24	Immediate early	ORFs m124, m124.1, and m125 located within the enhancer region are nonessential for MCMV growth <i>in vitro</i> (6)	
vMC137 vMC143 vMC149	m132_Ex1 m139 m145	C	sgg1	US22 (GF2)	24	Glycoprotein	Exon 2 of M133 (sgg1) (61, 73) US22 family homolog Downmodulates expression of cellular MULT-1 (60) and is a member of MGP family m145	
vMC152 vMC159	m148 m155				24	Glycoprotein	Member of MGP family m145 that modulates NK cell (inhibition) and T cell response and impedes an NKG2D ligand (H60) (41, 79)	
vMC163	m159	C			24	Putative membrane glycoprotein	Putative membrane glycoprotein	
vMC165 vMC172 vMC174	m161 m168 m170	C			24	Putative membrane glycoprotein	Glycoprotein m02 Glycoprotein m02 Glycoprotein m02	
vMC005	m05				48			
vMC012	m12				48			
vMC014	m14				48			

vMCO43	m39	C		48	Potential ORF located within the origin of replication (89)
vMCO66	m59	C	UL74 P	48	Functional homolog of HCMV gO, has key role in determining the entry pathway of MCMV (95)
vMCO73	m74	C		48	Potential alternative splice to M112 Ex1 (e1) (22), as found for HCMV UL112/
vMC108	M113		UL113 P	48	UL113 (115) Predicted MCMV homologue of HCMV spliced ORF m131/129 is a chemokine homolog and determinant of viral pathogenicity (35) and may modulate cytokine signaling (79)
vMC118	m119.3			48	
vMC133	m129	C		48	

^a Microarray probes for coding MCMV ORFs found to be significantly upregulated in MCMV-infected cells versus mock-infected cells to a high confidence level ($P \leq 0.05$ by empirical Bayes analysis).

^b Probe ID, probe identifier.

^c Time on, time detected.

^d a, amino acids; vICA, viral inhibitor of caspase-8 activation; vMIA, viral mitochondrial inhibitor of apoptosis; ER, endoplasmic reticulum; RIP1, receptor-interacting protein kinase 1; ssDNA, single-stranded DNA; PKR, protein kinase R; APCs, antigen-presenting cells; MGP, membrane glycoprotein; CTL, cytotoxic T lymphocyte; IFN- γ , gamma interferon; HHV-6, human herpesvirus 6.

^e Virion-associated proteins (VAPs), based on reference 49.

was performed based on a subset of 44 positive-control probes highly correlated across the data set (Pearson r of >0.90). Normalized expression data (see Table S3 in the supplemental material) were subjected to a statistically rigorous threshold detection methodology for providing on/off calls for each probe based on a receiver operating characteristic (ROC) (12). From these ROC analyses, we evaluated specificity levels corresponding to given sensitivities of 70%, 80%, and 90%. At a moderate sensitivity of 70%, we were able to obtain an average specificity of 93%, and this was chosen as affording an optimal balance between identifying true positives and excluding true negatives with stringency (for ROC plots, see Fig. S1 and S2 in the supplemental material). Accordingly, we detected 297 total probes having “on” calls and 163 probes for coding MCMV ORFs, making 87.6% of the MCMV genome detectable at 48 hpi (for a list of genes detected, see Table S4 in the supplemental material).

To account for experimental variation, statistical testing (empirical Bayes moderated t test) was applied between mock-infected and infected groups to identify differential expression of only the most highly significant MCMV ORFs. By use of this more stringent approach, 119 ORFs were found to be significantly activated to a confidence level of $P \leq 0.05$ above mock-infected levels at all time points (Table 1). These included the DNA polymerase subunit M54 (59), known inhibitors of major histocompatibility complex class I (MHC-I) surface expression m04 (gp34) (51) and m06 (gp48) (90), and the Fc receptor m138 (108). After a single round of replication at 24 hpi, a total of 111 MCMV ORFs were detected at the high significance level. To further validate these findings, a subset of MCMV ORFs were subjected to quantitative reverse transcription-PCR (qRT-PCR) analysis (for primer sequences, see File S1 in the supplemental material), and in agreement with the microarray results, each test case showed that ORF expression was also detectable by qRT-PCR (Fig. 1a).

As previously noted for HCMV microarray analysis, there is no overt positional bias toward expression of coding ORFs based on genomic location that could be linked to the patterns of gene expression observed during infection. MCMV ORFs were annotated based on Rawlinson et al. (89) and updated with details from additional publications wherever possible. MCMV ORFs from recent predictions (15, 105) were aligned against 55-mer probe sequences, identifying five probes overlapping with newly predicted ORFs (m107-m107.2, m16-m16.2, m22-m22.1, M34-m34.2, and M58-m58.1), which were reannotated accordingly.

As a result of the statistical cutoff ($P \leq 0.05$), MCMV probes for ORFs M44, M70, M75, m135, m143, m144, m153, and m157 failed to be included, although these genes have been reported to be expressed in previous MCMV studies or are homologues of HCMV genes reported to be expressed (21, 29, 34, 79, 80, 89, 92, 110, 118). It is most likely that the specific probes for these genes exhibit false-negative results. Nevertheless, in this study, we aimed to purposefully avoid false positives at the sacrifice of capturing a modest level of false negatives. For this reason, we also did not detect *ie1* or *ie3* expression until 24 hpi based on the statistical cutoff; however, these genes are detectable as early as 0.5 hpi and 2.5 hpi by use of a more sensitive qRT-PCR approach (see Fig. S3 in the supplemental material).

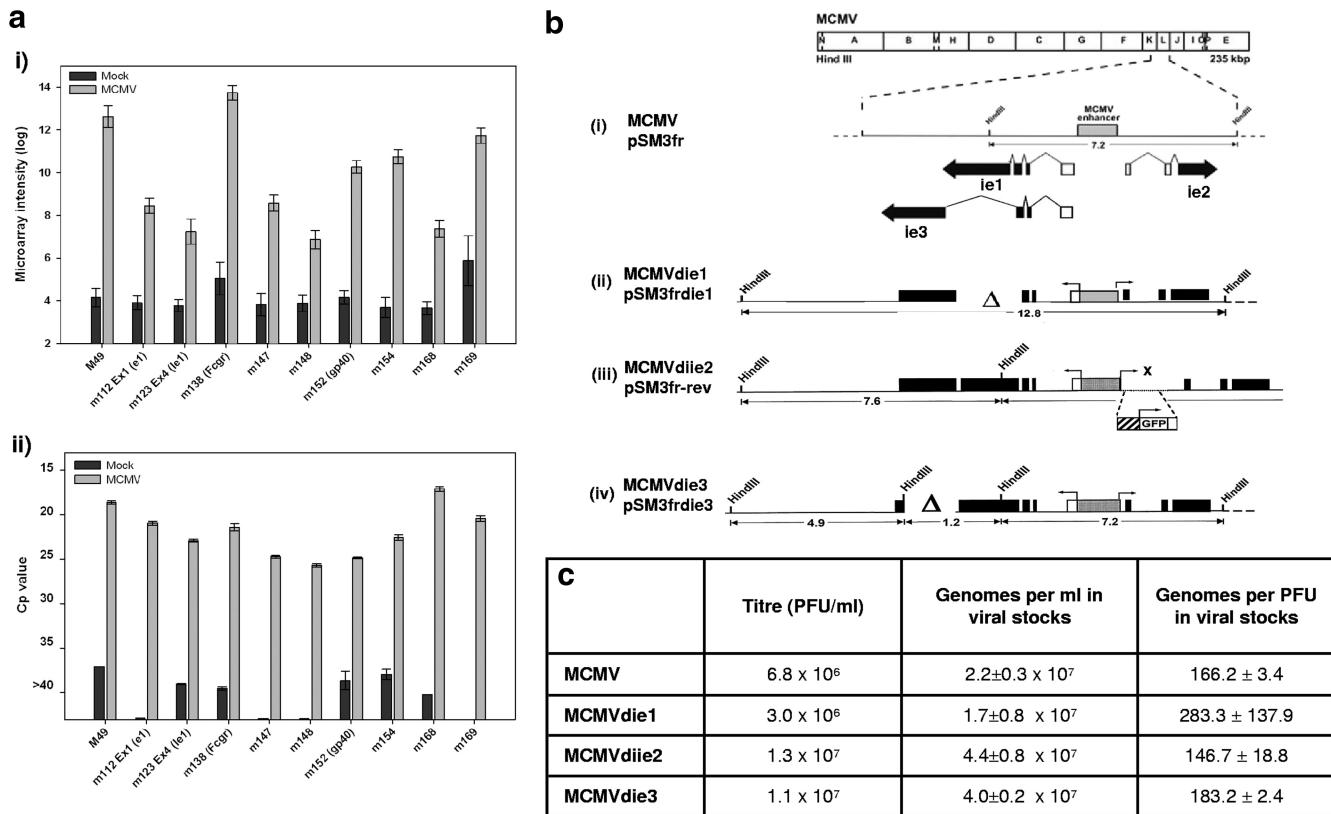


FIG. 1. MCMV ORF detection and characterization of MCMV IE deletion mutant strains. (a) (Panel i) Microarray signals for 10 MCMV ORFs in mock- and MCMV-infected cells. (Panel ii) qRT-PCR validation of the 10 MCMV ORFs at 24 hpi. The y axis represents crossing point (Cp) values from qPCR amplification curves, with low Cp values indicating high transcript abundance. Error bars represent standard errors of the mean. (b) Schematic representations of recombinant MCMV IE deletion mutants. The map of the parental MCMV genome is shown at the top, with structures of the *ie1*, *ie2*, and *ie3* transcripts below. Coding exons are shown in black, with arrows indicating the directions of transcription, and white triangles represent deleted loci. The gray box marks the MCMV *ie1/ie3* promoter enhancer (MIEP). (Line iii) The MCMVdie3 revertant strain was renamed MCMVdie2 in this study, as the HCMV MIEP is inserted between two HpaI sites spanning the transcription start site of the *ie2* gene, disrupting *ie2* expression (marked with \times). GFP, green fluorescent protein. (c) Viral titers and genome particle/PFU equivalences of the four MCMV strains, as determined by qPCR.

To gain further insight into the transcriptional programming of MCMV, we next sought to profile gene expression from three well-characterized MCMV mutants (5, 23, 36, 72) alongside the parental MCMV strain (111) (for schematics of strains, see Fig. 1b). To characterize the mutant strains before microarray analysis, we sought to (i) determine equivalent infectious doses at the genomic level by measuring genome/PFU ratio for each stock, (ii) ensure that generating the *ie3* deletion mutant (MCMVdie3) in a complementing cell line did not drastically alter the infectious-particle ratio, (iii) ensure that viral growth phenotypes were consistent with those previously published (5, 36, 72), and (iv) ensure that no viral transcription was occurring from deleted loci. On the basis of quantitative PCR (qPCR), we detected equivalent numbers of MCMV genome copies per PFU for each viral strain (Fig. 1c), using as a calibrator a reference plasmid containing the m115 (gL) gene (nucleotides [nt] 166387 to 167208; GenBank accession no. NC_004065) (for a detailed account of this approach, see reference 98). Equivalent numbers of MCMV genomes were also found at 2 hpi inside cells infected with different MCMV strains (data not shown). Multistep growth curves confirmed viral growth phenotypes (see Fig. S4 in the supplemental ma-

terial), and qRT-PCR (Qiagen 1-step kit; Germany) confirmed that transcription was not detectable from the respective deleted loci for *ie1*, *ie2*, and *ie3* (data not shown). These data show that the four MCMV strains are experimentally comparable for downstream gene expression analysis.

Based on previous virologic characterization of these MCMV immediate-early (IE) mutants, we expected to observe different gene expression profiles for the MCMV strains. For example, given that removal of the *ie2* gene causes no reported change in phenotype (45), we anticipated few gene expression changes in the MCMVdie2 strain relative to the parental MCMV strain. Alternatively, given that *ie3* has an indispensable regulatory function and is essential for viral growth (5), we expected little or no viral gene expression to be detectable from the MCMVdie3 strain. However, for the *ie1* deletion mutant (MCMVdie1), the expectation was less clear, given that this strain has wild-type growth characteristics and yet the IE1 protein is well known to have transcriptional regulatory activity (24, 39, 76) and is further known to interact with cellular host factors (81, 104). In order to profile the gene expression of each mutant strain, we infected NIH 3T3 fibroblasts in parallel at an MOI of 1 and harvested total RNA for microarray anal-

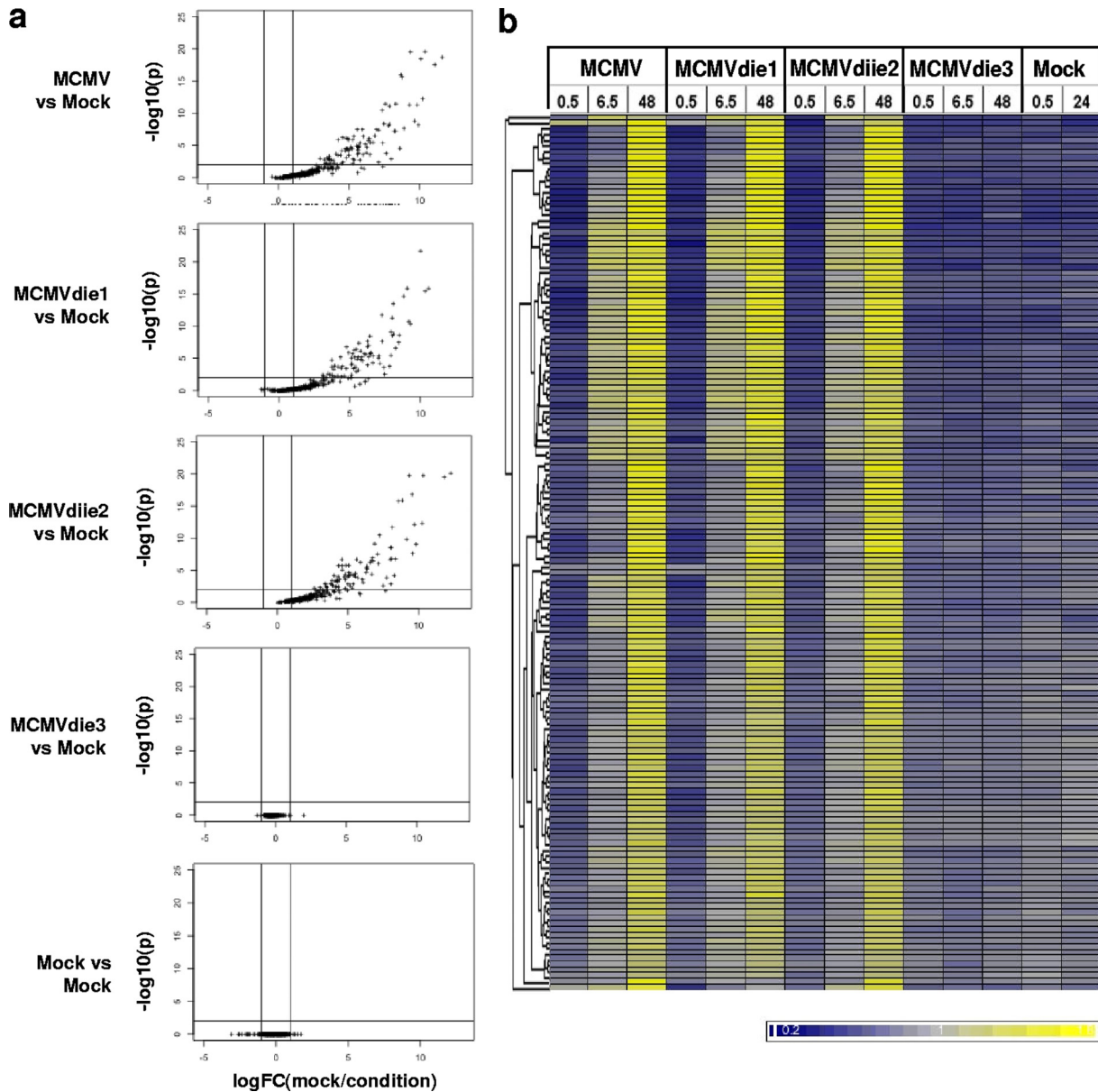


FIG. 2. Gene expression program of MCMV, MCMVdie1, MCMVdie2, and MCMVdie3. (a) Volcano plots comparing microarray signals from mock-infected and infected samples at 48 hpi, using P value (y axis) and fold change (FC) (x axis) comparisons derived from empirical Bayes testing, with two biological replicates per group. (b) Hierarchical clustering of high-confidence MCMV probes, with each row representing a single probe normalized to its mean value across the data set to show relative expression. Yellow indicates increased expression and blue indicates decreased expression relative to the mean. Genes clustered based on the similarity of their expression profiles across the data set, with similar genes connected at the hierarchical tree on the left. Data represent mean values from two biological replicates. Numerical values at top indicate hours postinfection.

ysis at 0.5, 6.5, and 48 hpi, along with that of mock-infected cells.

Figure 2 shows the comparative activation of viral transcriptomes among the four MCMV strains at 48 hpi and indicates that the transcriptomes of MCMVdie1 and MCMVdie2 are activated with profiles of viral gene expression very similar to that of the parental MCMV strain over the 48-h period (Fig. 2a). Similar numbers (within 10%) of MCMV probes were detectable from MCMVdie1 (103 ORFs), MCMVdie2 (114 ORFs), and the parental strain (113 ORFs) at 48 hpi. The degree of similarity in

expression profiles among the MCMVdie1, MCMVdie2, and parental MCMV strains suggests that *ie1* and *ie2* have a redundant or negligible transcriptional regulatory role in controlling downstream MCMV gene expression during fibroblast infection. Hierarchical clustering (Fig. 2b) further indicates few, if any, differences in the global gene expression profiles of MCMVdie1 and MCMVdie2 compared to that of the parental MCMV strain. These results could point to a redundant role for the *ie1* and *ie2* genes in controlling downstream viral gene expression or, alternatively, a lack of

TABLE 2. High-confidence MCMV microarray antisense probes^a

Unique probe ID ^b	ORF	Time on ^c (hpi)	Details of cDNA cloning validation	Sense probe ^d
vMC336	m148as	6.5	Validated with AS cDNA clone L151 at nt 208012 to 207467 (5' to 3'), overlapping m148 (AS) and m149 (S); clone length, 545 nt	S
vMC357	m169as	6.5		S
vMC175	m05as	24		S
vMC180	m163as	24		S
vMC188	m04as	24	Validated with AS cDNA clone IE150 at nt 4043 to 3943 (5' to 3'), overlapping m04 (AS); clone length, 384 nt	S
vMC189	m05as	24		S
vMC190	m06as	24		S
vMC191	m07as	24		
vMC193	m09as	24		
vMC197	m13as	24		S
vMC229	m41as	24		S
vMC236	M47as	24		
vMC241	M50as	24		S
vMC248	M57as	24		S
vMC257	m74as	24	Validated with AS cDNA clone L147 at nt 104825 to 105449 (5' to 3'), overlapping m74 (AS); clone length, 624 nt	S
vMC269	M87as	24		
vMC270	M88as	24		S
vMC283	M102as	24		S
vMC285	M104as	24		
vMC291	M113as	24		S
vMC293	M115as	24		S
vMC299	m119.2as	24		S
vMC311	m124as	24		S
vMC333	m145as	24		S
vMC335	m147as	24		
vMC351	m163as	24		S
vMC356	m168as	24		S
vMC239	M48as	48		S
vMC251	m69.1as	48		
vMC272	M89 Ex2as	48		
vMC277	M94as	48	Validated with AS cDNA clone L164 at nt 137299 to 137096 (5' to 3'), overlapping m94 (AS); clone length, 203 nt	S
vMC289	m108as	48		S
vMC300	m119.3as	48		S
vMC319	m132 Ex2as	48		S
vMC332	m144	48		

^a Microarray probes for antisense transcripts found to be significantly upregulated in MCMV-infected cells versus mock-infected cells to a high confidence level ($P \leq 0.05$ by empirical Bayes analysis).

^b Probe ID, probe identifier.

^c Time on, time detected.

^d AS probes with significant signal also found from the corresponding sense probes are marked with an "S."

sensitivity in controlling the viral genomic program in fully permissive fibroblasts.

In marked contrast to the *ie1* and *ie2* mutant strains, MCMV*die3* exhibited an undetectable level of viral gene expression, suggesting that *ie3* acts as a global *trans*-activator of downstream MCMV gene expression, as indicated by previous studies (5). To further examine the transcriptional status of MCMV*die3* using a more sensitive approach, IE and downstream MCMV genes were measured using qRT-PCR in MCMV*die3*-infected cells both in the presence and in the absence of 50 µg/ml cycloheximide (C7698; Sigma, United Kingdom) at 2.5 hpi. These experiments confirmed that IE kinetic class genes were expressed in MCMV*die3* but that genes beyond the IE region were not (see Fig. S5 in the supplemental material).

The design of the MCMV microarray platform enables selective detection of transcripts originating from both strands of the viral genome by having probes designed in sense (S) and antisense (AS) orientations to each MCMV ORF. At 24 hpi,

we detected antisense transcripts from 23 AS loci, five of which (m104as, M113as, m147as, m163as, and m168as) have overlapping ORFs on the opposite strand of the genome, indicating known or predicted regions of bidirectional transcription based on prior annotation (105). Three other loci were found to have neighboring but nonoverlapping ORFs in their vicinity (M57as, m74as, and M88as). An additional 15 MCMV AS probes detected at 24 hpi were found to have no overlapping or nearby ORFs located on the opposite strand, indicating previously unknown noncoding transcripts derived from regions outside MCMV ORFs (m04as, m05as, m06as, m07as, m09as, m13as, m41as, M47as, M50as, M87as, M102as, M115as, m119.2as, m124as, and m145as). At 48 hpi, an additional eight antisense probes were detectable, but all have overlapping or nearby ORFs on the opposite strand of the genome (M48as, m69.1as, M89as, M94as, m108as, m119.3as, m132as, and m144as). In total, evidence of antisense transcription was detected from 35 loci over the four time points as measured by microarray analysis (Table 2 and Fig. 3). Twenty-six of these loci were also

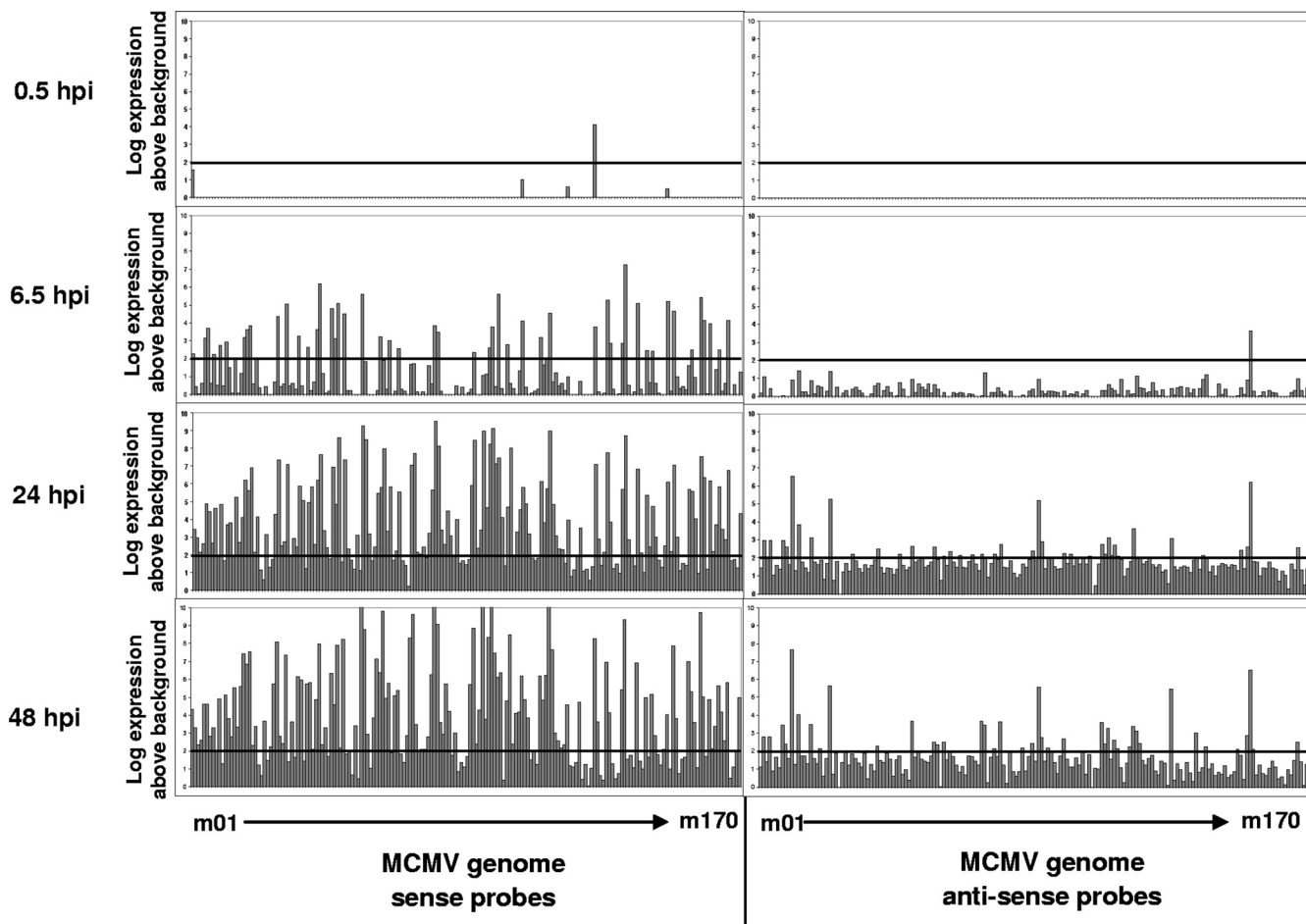


FIG. 3. MCMV genome activation measured by microarray analysis and qRT-PCR. Transcript abundance of ORFs expressed from the parental MCMV strain was measured using oligonucleotide microarrays at 0.5, 6.5, 24, and 48 hpi in NIH 3T3 cells at an MOI of 1. Histograms represent mean values from two replicate samples after background (mock infection) subtraction. Transcripts are arranged in order from left to right according to ORF names ranging from m01 to m170, with sense probes shown on the left and antisense probes on the right. All raw data are available in the supplemental material.

found to have significant signal from the corresponding sense (S) probe, indicating a potential site of bidirectional transcription. A trend toward antisense transcription occurring more frequently at the terminal ends of the MCMV genome is also noted (Fig. 3).

In order to independently validate AS transcripts identified by microarray analysis, we generated cDNA libraries from MCMV-infected fibroblasts pooled from 4, 8, and 12 hpi (IE library), 16, 24, and 32 hpi (E library), or 40, 60, 80, and 100 hpi (L library). cDNA libraries were generated as described previously for HCMV (120). cDNA clones overlapping AS microarray regions were found at m04as, m74as, M94as (none of which have overlapping ORFs on the opposite strand of the genome), and m148as (which has the m147 ORF on the opposite strand of the genome) (for validated AS transcripts, see Table 2). We also found one large cDNA clone that overlapped three MCMV ORFs (m119.2, m119.3, and m119.4), two of which had potential AS regions identified by microarray probes (m119.2 and m119.3). Four additional AS cDNA clones were found to overlap AS regions not identified by microarray analysis (m19as, M72as, m149as, and m151as). These experi-

ments thus reveal for the first time that antisense transcription occurs frequently throughout the MCMV genome, an observation that will likely seed further studies.

This work was supported by Wellcome Trust Programme grant no. WT 066784/Z/02/Z (to P.G.), Unity through Knowledge Fund grant no. UKF 08/07 (to J.T.), and Ministerio de Educación y Ciencia grant no. SAF 2008 00382 (to A.A.). qPCR data were obtained in the Kinetic Parameter Facility of The Centre for Systems Biology at Edinburgh, which is a Centre for Integrative Systems Biology (CISB) funded by BBSRC and EPSRC BB/D019621/1 (P.G.).

We kindly thank Ulrich Koszinowski for his comments and input on the manuscript. We also thank Daniel Foster and Fátima García del Rey for their technical input, Stipan Jonjic for his support in generating cDNA libraries, and Chitrangada Das Mukhopadhyay for bioinformatics analysis of MCMV cDNA clones.

REFERENCES

1. Abate, D. A., S. Watanabe, and E. S. Mocarski. 2004. Major human cytomegalovirus structural protein pp65 (ppUL83) prevents interferon response factor 3 activation in the interferon response. *J. Virol.* **78**:10995–11006.
2. Abenes, G., et al. 2001. Murine cytomegalovirus open reading frame M27 plays an important role in growth and virulence in mice. *J. Virol.* **75**:1697–1707.

3. **Anders, D. G.** 1990. Nucleotide sequence of a cytomegalovirus single-stranded DNA-binding protein gene: comparison with alpha- and gamma-herpesvirus counterparts reveals conserved segments. *J. Gen. Virol.* **71**(Pt. 10):2451–2456.
4. **Anders, D. G., and W. Gibson.** 1988. Location, transcript analysis, and partial nucleotide sequence of the cytomegalovirus gene encoding an early DNA-binding protein with similarities to ICP8 of herpes simplex virus type 1. *J. Virol.* **62**:1364–1372.
5. **Angulo, A., P. Ghazal, and M. Messerle.** 2000. The major immediate-early gene ie3 of mouse cytomegalovirus is essential for viral growth. *J. Virol.* **74**:11129–11136.
6. **Angulo, A., M. Messerle, U. H. Koszinowski, and P. Ghazal.** 1998. Enhancer requirement for murine cytomegalovirus growth and genetic complementation by the human cytomegalovirus enhancer. *J. Virol.* **72**:8502–8509.
7. **Arai, Y., et al.** 2003. Neuron-specific activation of murine cytomegalovirus early gene e1 promoter in transgenic mice. *Am. J. Pathol.* **163**:643–652.
8. **Arapovic, J., T. Lenac Rovis, A. B. Reddy, A. Krmpotic, and S. Jonjic.** 2009. Promiscuity of MCMV immunoevasin of NKG2D: m138/fcr-1 down-modulates RAE-1epsilon in addition to MULT-1 and H60. *Mol. Immunol.* **47**:114–122.
9. **Baldick, C. J., Jr., and T. Shenk.** 1996. Proteins associated with purified human cytomegalovirus particles. *J. Virol.* **70**:6097–6105.
10. **Baluchova, K., M. Kirby, M. M. Ahasan, and C. Sweet.** 2008. Preliminary characterization of murine cytomegaloviruses with insertional and deleterial mutations in the M34 open reading frame. *J. Med. Virol.* **80**:1233–1242.
11. **Baum, E. Z., et al.** 1993. Expression and analysis of the human cytomegalovirus UL80-encoded protease: identification of autoproteolytic sites. *J. Virol.* **67**:497–506.
12. **Bilban, M., L. K. Buehler, S. Head, G. Desoye, and V. Quaranta.** 2002. Defining signal thresholds in DNA microarrays: exemplary application for invasive cancer. *BMC Genomics* **3**:19.
13. **Bogner, E., M. Reschke, B. Reis, T. Mockenhaupt, and K. Radsak.** 1993. Identification of the gene product encoded by ORF UL56 of the human cytomegalovirus genome. *Virology* **196**:290–293.
14. **Borst, E. M., S. Mathys, M. Wagner, W. Muranyi, and M. Messerle.** 2001. Genetic evidence of an essential role for cytomegalovirus small capsid protein in viral growth. *J. Virol.* **75**:1450–1458.
15. **Broccieri, L., T. N. Kledal, S. Karlin, and E. S. Mocarski.** 2005. Predicting coding potential from genome sequence: application to betaherpesviruses infecting rats and mice. *J. Virol.* **79**:7570–7596.
16. **Browne, E. P., and T. Shenk.** 2003. Human cytomegalovirus UL83-coded pp65 virion protein inhibits antiviral gene expression in infected cells. *Proc. Natl. Acad. Sci. U. S. A.* **100**:11439–11444.
17. **Brune, W., C. Menard, J. Heesemann, and U. H. Koszinowski.** 2001. A ribonuclease reductase homolog of cytomegalovirus and endothelial cell tropism. *Science* **291**:303–305.
18. **Bubeck, A., et al.** 2002. The glycoprotein gp48 of murine cytomegalovirus: proteasome-dependent cytosolic dislocation and degradation. *J. Biol. Chem.* **277**:2216–2224.
19. **Buck, A. H., et al.** 2010. Post-transcriptional regulation of miR-27 in murine cytomegalovirus infection. *RNA* **16**:307–315.
20. **Buck, A. H., et al.** 2007. Discrete clusters of virus-encoded microRNAs are associated with complementary strands of the genome and the 7.2-kilobase stable intron in murine cytomegalovirus. *J. Virol.* **81**:13761–13770.
21. **Budt, M., L. Niederstadt, R. S. Valchanova, S. Jonjic, and W. Brune.** 2009. Specific inhibition of the PKR-mediated antiviral response by the murine cytomegalovirus proteins m142 and m143. *J. Virol.* **83**:1260–1270.
22. **Buhler, B., G. M. Keil, F. Weiland, and U. H. Koszinowski.** 1990. Characterization of the murine cytomegalovirus early transcription unit e1 that is induced by immediate-early proteins. *J. Virol.* **64**:1907–1919.
23. **Busche, A., A. Angulo, P. Kay-Jackson, P. Ghazal, and M. Messerle.** 2008. Phenotypes of major immediate-early gene mutants of mouse cytomegalovirus. *Med. Microbiol. Immunol.* **197**:233–240.
24. **Cardin, R. D., G. B. Abenes, C. A. Stoddart, and E. S. Mocarski.** 1995. Murine cytomegalovirus IE2, an activator of gene expression, is dispensable for growth and latency in mice. *Virology* **209**:236–241.
25. **Chee, M., S. A. Rudolph, B. Plachter, B. Barrell, and G. Jahn.** 1989. Identification of the major capsid protein gene of human cytomegalovirus. *J. Virol.* **63**:1345–1353.
26. **Chee, M. S., et al.** 1990. Analysis of the protein-coding content of the sequence of human cytomegalovirus strain AD169. *Curr. Top. Microbiol. Immunol.* **154**:125–169.
27. **Cicin-Sain, L., et al.** 2008. Dominant-negative FADD rescues the in vivo fitness of a cytomegalovirus lacking an antiapoptotic viral gene. *J. Virol.* **82**:2056–2064.
28. **Corbett, A. J., C. A. Forbes, D. Moro, and A. A. Scalzo.** 2007. Extensive sequence variation exists among isolates of murine cytomegalovirus within members of the m02 family of genes. *J. Gen. Virol.* **88**:758–769.
29. **Crane, M. P., et al.** 1986. Identification of the human cytomegalovirus glycoprotein B gene and induction of neutralizing antibodies via its expression in recombinant vaccinia virus. *EMBO J.* **5**:3057–3063.
30. **Cranmer, L. D., C. Clark, and D. H. Spector.** 1994. Cloning, characterization, and expression of the murine cytomegalovirus homologue of the human cytomegalovirus 28-kDa matrix phosphoprotein (UL99). *Virology* **205**:417–429.
31. **Crnkovic-Mertens, I., et al.** 1998. Virus attenuation after deletion of the cytomegalovirus Fc receptor gene is not due to antibody control. *J. Virol.* **72**:1377–1382.
32. **Dallas, P. B., P. A. Lyons, J. B. Hudson, A. A. Scalzo, and G. R. Shellam.** 1994. Identification and characterization of a murine cytomegalovirus gene with homology to the UL25 open reading frame of human cytomegalovirus. *Virology* **200**:643–650.
33. **Dolkens, L., et al.** 2007. Mouse cytomegalovirus microRNAs dominate the cellular small RNA profile during lytic infection and show features of posttranscriptional regulation. *J. Virol.* **81**:13771–13782.
34. **Ertl, P. F., and K. L. Powell.** 1992. Physical and functional interaction of human cytomegalovirus DNA polymerase and its accessory protein (ICP36) expressed in insect cells. *J. Virol.* **66**:4126–4133.
35. **Fleming, P., et al.** 1999. The murine cytomegalovirus chemokine homolog, m131/129, is a determinant of viral pathogenicity. *J. Virol.* **73**:6800–6809.
36. **Ghazal, P., et al.** 2005. Elimination of ie1 significantly attenuates murine cytomegalovirus virulence but does not alter replicative capacity in cell culture. *J. Virol.* **79**:7182–7194.
37. **Goldmacher, V. S., et al.** 1999. A cytomegalovirus-encoded mitochondrial inhibitor of apoptosis structurally unrelated to Bcl-2. *Proc. Natl. Acad. Sci. U. S. A.* **96**:12536–12541.
38. **Gompels, U. A., et al.** 1995. The DNA sequence of human herpesvirus-6: structure, coding content, and genome evolution. *Virology* **209**:29–51.
39. **Gribaudo, G., et al.** 1996. The murine cytomegalovirus immediate-early 1 protein stimulates NF-kappa B activity by transactivating the NF-kappa B p105/p50 promoter. *Virus Res.* **45**:15–27.
40. **Gutermann, A., et al.** 2002. Strategies for the identification and analysis of viral immune-evasive genes—cytomegalovirus as an example. *Curr. Top. Microbiol. Immunol.* **269**:1–22.
41. **Hasan, M., et al.** 2005. Selective down-regulation of the NKG2D ligand H60 by mouse cytomegalovirus m155 glycoprotein. *J. Virol.* **79**:2920–2930.
42. **Hayashi, M. L., C. Blankenship, and T. Shenk.** 2000. Human cytomegalovirus UL69 protein is required for efficient accumulation of infected cells in the G1 phase of the cell cycle. *Proc. Natl. Acad. Sci. U. S. A.* **97**:2692–2696.
43. **Hengel, H., et al.** 1999. Cytomegaloviral control of MHC class I function in the mouse. *Immunol. Rev.* **168**:167–176.
44. **Holtappels, R., N. K. Grzimek, D. Thomas, and M. J. Reddehase.** 2002. Early gene m18, a novel player in the immune response to murine cytomegalovirus. *J. Gen. Virol.* **83**:311–316.
45. **Holtappels, R., et al.** 2008. Subdominant CD8 T-cell epitopes account for protection against cytomegalovirus independent of immunodomination. *J. Virol.* **82**:5781–5796.
46. **Holtappels, R., et al.** 2000. The putative natural killer decoy early gene m04 (gp34) of murine cytomegalovirus encodes an antigenic peptide recognized by protective antiviral CD8 T cells. *J. Virol.* **74**:1871–1884.
47. **Jahn, G., et al.** 1987. Map position and nucleotide sequence of the gene for the large structural phosphoprotein of human cytomegalovirus. *J. Virol.* **61**:1358–1367.
48. **Jahn, G., B. C. Scholl, B. Traupe, and B. Fleckenstein.** 1987. The two major structural phosphoproteins (pp65 and pp150) of human cytomegalovirus and their antigenic properties. *J. Gen. Virol.* **68**(Pt. 5):1327–1337.
49. **Kattenhorn, L. M., et al.** 2004. Identification of proteins associated with murine cytomegalovirus virions. *J. Virol.* **78**:11187–11197.
50. **Kavanagh, D. G., and A. B. Hill.** 2001. Evasion of cytotoxic T lymphocytes by murine cytomegalovirus. *Semin. Immunol.* **13**:19–26.
51. **Kavanagh, D. G., U. H. Koszinowski, and A. B. Hill.** 2001. The murine cytomegalovirus immune evasion protein m4/gp34 forms biochemically distinct complexes with class I MHC at the cell surface and in a pre-Golgi compartment. *J. Immunol.* **167**:3894–3902.
52. **Kaye, J. F., U. A. Gompels, and A. C. Minson.** 1992. Glycoprotein H of human cytomegalovirus (HCMV) forms a stable complex with the HCMV UL115 gene product. *J. Gen. Virol.* **73**(Pt. 10):2693–2698.
53. **Keil, G. M., A. Ebeling-Keil, and U. H. Koszinowski.** 1987. Immediate-early genes of murine cytomegalovirus: location, transcripts, and translation products. *J. Virol.* **61**:526–533.
54. **Keil, G. M., A. Ebeling-Keil, and U. H. Koszinowski.** 1987. Sequence and structural organization of murine cytomegalovirus immediate-early gene 1. *J. Virol.* **61**:1901–1908.
55. **Keil, G. M., A. Ebeling-Keil, and U. H. Koszinowski.** 1984. Temporal regulation of murine cytomegalovirus transcription and mapping of viral RNA synthesized at immediate early times after infection. *J. Virol.* **50**:784–795.
56. **Khan, S., A. Zimmermann, M. Basler, M. Groettrup, and H. Hengel.** 2004. A cytomegalovirus inhibitor of gamma interferon signaling controls immunoproteasome induction. *J. Virol.* **78**:1831–1842.
57. **Kielczewska, A., et al.** 2009. Ly49P recognition of cytomegalovirus-infected

- cells expressing H2-Dk and CMV-encoded m04 correlates with the NK cell antiviral response. *J. Exp. Med.* **206**:515–523.
58. Kouzarides, T., A. T. Bankier, S. C. Satchwell, E. Preddy, and B. G. Barrell. 1988. An immediate early gene of human cytomegalovirus encodes a potential membrane glycoprotein. *Virology* **165**:151–164.
 59. Kouzarides, T., et al. 1987. Sequence and transcription analysis of the human cytomegalovirus DNA polymerase gene. *J. Virol.* **61**:125–133.
 60. Krmpotic, A., et al. 2005. NK cell activation through the NKG2D ligand MULT-1 is selectively prevented by the glycoprotein encoded by mouse cytomegalovirus gene m145. *J. Exp. Med.* **201**:211–220.
 61. Lagenaar, L. A., W. C. Manning, J. Vieira, C. L. Martens, and E. S. Mocarski. 1994. Structure and function of the murine cytomegalovirus sgg1 gene: a determinant of viral growth in salivary gland acinar cells. *J. Virol.* **68**:7717–7727.
 62. Leatham, M. P., P. R. Witte, and M. F. Stinski. 1991. Alternate promoter selection within a human cytomegalovirus immediate-early and early transcription unit (UL119–115) defines true late transcripts containing open reading frames for putative viral glycoproteins. *J. Virol.* **65**:6144–6153.
 63. Lee, M., et al. 2000. Murine cytomegalovirus containing a mutation at open reading frame M37 is severely attenuated in growth and virulence in vivo. *J. Virol.* **74**:11099–11107.
 64. Lemmermann, N. A., et al. 2010. Immune evasion proteins of murine cytomegalovirus preferentially affect cell surface display of recently generated peptide presentation complexes. *J. Virol.* **84**:1221–1236.
 65. Lenac, T., et al. 2006. The herpesviral Fc receptor fcr-1 down-regulates the NKG2D ligands MULT-1 and H60. *J. Exp. Med.* **203**:1843–1850.
 66. Li, W., K. Eidman, R. C. Gehrz, and B. Kari. 1995. Identification and molecular characterization of the murine cytomegalovirus homolog of the human cytomegalovirus UL100 gene. *Virus Res.* **36**:163–175.
 67. Littler, E., A. D. Stuart, and M. S. Chee. 1992. Human cytomegalovirus UL97 open reading frame encodes a protein that phosphorylates the anti-viral nucleoside analogue ganciclovir. *Nature* **358**:160–162.
 68. Loewendorf, A., et al. 2004. Identification of a mouse cytomegalovirus gene selectively targeting CD86 expression on antigen-presenting cells. *J. Virol.* **78**:13062–13071.
 69. Loutsch, J. M., N. J. Galvin, M. L. Bryant, and B. C. Holwerda. 1994. Cloning and sequence analysis of murine cytomegalovirus protease and capsid assembly protein genes. *Biochem. Biophys. Res. Commun.* **203**:472–478.
 70. Lyons, P. A., P. B. Dallas, C. Carrello, G. R. Shellam, and A. A. Scalzo. 1994. Mapping and transcriptional analysis of the murine cytomegalovirus homologue of the human cytomegalovirus UL103 open reading frame. *Virology* **204**:835–839.
 71. Mack, C., A. Sickmann, D. Lembo, and W. Brune. 2008. Inhibition of proinflammatory and innate immune signaling pathways by a cytomegalovirus RIP1-interacting protein. *Proc. Natl. Acad. Sci. U. S. A.* **105**:3094–3099.
 72. Manning, W. C., and E. S. Mocarski. 1988. Insertional mutagenesis of the murine cytomegalovirus genome: one prominent alpha gene (ie2) is dispensable for growth. *Virology* **167**:477–484.
 73. Manning, W. C., C. A. Stoddart, L. A. Lagenaar, G. B. Abenes, and E. S. Mocarski. 1992. Cytomegalovirus determinant of replication in salivary glands. *J. Virol.* **66**:3794–3802.
 74. Marshall, E. E., and A. P. Geballe. 2009. Multifaceted evasion of the interferon response by cytomegalovirus. *J. Interferon Cytokine Res.* **29**: 609–619.
 75. Menard, C., et al. 2003. Role of murine cytomegalovirus US22 gene family members in replication in macrophages. *J. Virol.* **77**:5557–5570.
 76. Messerle, M., B. Buhler, G. M. Keil, and U. H. Koszinowski. 1992. Structural organization, expression, and functional characterization of the murine cytomegalovirus immediate-early gene 3. *J. Virol.* **66**:27–36.
 77. Messerle, M., G. M. Keil, and U. H. Koszinowski. 1991. Structure and expression of murine cytomegalovirus immediate-early gene 2. *J. Virol.* **65**:1638–1643.
 78. Meyer, H., et al. 1988. Identification and procarciotic expression of the gene coding for the highly immunogenic 28-kilodalton structural phosphoprotein (pp28) of human cytomegalovirus. *J. Virol.* **62**:2243–2250.
 79. Mocarski, E. S., Jr. 2004. Immune escape and exploitation strategies of cytomegaloviruses: impact on and imitation of the major histocompatibility system. *Cell. Microbiol.* **6**:707–717.
 80. Mocarski, E. S., Jr. 2002. Immunomodulation by cytomegaloviruses: manipulative strategies beyond evasion. *Trends Microbiol.* **10**:332–339.
 81. Munch, K., M. Messerle, B. Plachter, and U. H. Koszinowski. 1992. An acidic region of the 89K murine cytomegalovirus immediate early protein interacts with DNA. *J. Gen. Virol.* **73**(Pt. 3):499–506.
 82. Muranyi, W., J. Haas, M. Wagner, G. Krohne, and U. H. Koszinowski. 2002. Cytomegalovirus recruitment of cellular kinases to dissolve the nuclear lamina. *Science* **297**:854–857.
 83. Oliveira, S. A., and T. E. Shenk. 2001. Murine cytomegalovirus M78 protein, a G protein-coupled receptor homologue, is a constituent of the virion and facilitates accumulation of immediate-early viral mRNA. *Proc. Natl. Acad. Sci. U. S. A.* **98**:3237–3242.
 84. Pinto, A. K., A. M. Jamieson, D. H. Raulet, and A. B. Hill. 2007. The role of NKG2D signaling in inhibition of cytotoxic T-lymphocyte lysis by the murine cytomegalovirus immunoevasin m152/gp40. *J. Virol.* **81**:12564–12571.
 85. Preston, V. G., J. W. Palfreyman, and B. M. Dutia. 1984. Identification of a herpes simplex virus type 1 polypeptide which is a component of the virus-induced ribonucleotide reductase. *J. Gen. Virol.* **65**(Pt. 9):1457–1466.
 86. Pyles, R. B., N. M. Sawtell, and R. L. Thompson. 1992. Herpes simplex virus type 1 dUTPase mutants are attenuated for neurovirulence, neuroinvasiveness, and reactivation from latency. *J. Virol.* **66**:6706–6713.
 87. Rapp, M., et al. 1992. Identification of the murine cytomegalovirus glycoprotein B gene and its expression by recombinant vaccinia virus. *J. Virol.* **66**:4399–4406.
 88. Rawlinson, W. D., and B. G. Barrell. 1993. Spliced transcripts of human cytomegalovirus. *J. Virol.* **67**:5502–5513.
 89. Rawlinson, W. D., H. E. Farrell, and B. G. Barrell. 1996. Analysis of the complete DNA sequence of murine cytomegalovirus. *J. Virol.* **70**:8833–8849.
 90. Reusch, U., et al. 1999. A cytomegalovirus glycoprotein re-routes MHC class I complexes to lysosomes for degradation. *EMBO J.* **18**:1081–1091.
 91. Ruger, B., et al. 1987. Primary structure and transcription of the genes coding for the two virion phosphoproteins pp65 and pp71 of human cytomegalovirus. *J. Virol.* **61**:446–453.
 92. Saederup, N., and E. S. Mocarski, Jr. 2002. Fatal attraction: cytomegalovirus-encoded chemokine homologs. *Curr. Top. Microbiol. Immunol.* **269**: 235–256.
 93. Scalzo, A. A., C. A. Forbes, N. J. Davis-Poynter, H. E. Farrell, and P. A. Lyons. 1995. DNA sequence and transcriptional analysis of the glycoprotein M gene of murine cytomegalovirus. *J. Gen. Virol.* **76**(Pt. 11):2895–2901.
 94. Schnee, M., Z. Ruzsics, A. Bubeck, and U. H. Koszinowski. 2006. Common and specific properties of herpesvirus UL34/UL31 protein family members revealed by protein complementation assay. *J. Virol.* **80**:11658–11666.
 95. Serivano, L., et al. 2010. The m74 gene product of murine cytomegalovirus (MCMV) is a functional homolog of human CMV gO and determines the entry pathway of MCMV. *J. Virol.* **84**:4469–4480.
 96. Sharp, E. L., N. J. Davis-Poynter, and H. E. Farrell. 2009. Analysis of the subcellular trafficking properties of murine cytomegalovirus M78, a 7 transmembrane receptor homologue. *J. Gen. Virol.* **90**:59–68.
 97. Sherman, G., J. Gottlieb, and M. D. Challberg. 1992. The UL8 subunit of the herpes simplex virus helicase-primase complex is required for efficient primer utilization. *J. Virol.* **66**:4884–4892.
 98. Simon, C. O., C. K. Seckert, D. Dreis, M. J. Reddehase, and N. K. Grzimek. 2005. Role for tumor necrosis factor alpha in murine cytomegalovirus transcriptional reactivation in latently infected lungs. *J. Virol.* **79**:326–340.
 99. Singh, R., E. Haghjoo, and F. Liu. 2003. Cytomegalovirus M43 gene modulates T helper cell response. *Immunol. Lett.* **88**:31–35.
 100. Skaletskaya, A., et al. 2001. A cytomegalovirus-encoded inhibitor of apoptosis that suppresses caspase-8 activation. *Proc. Natl. Acad. Sci. U. S. A.* **98**:7829–7834.
 101. Spaete, R. R., R. C. Gehrz, and M. P. Landini. 1994. Human cytomegalovirus structural proteins. *J. Gen. Virol.* **75**(Pt. 12):3287–3308.
 102. Sullivan, V., et al. 1992. A protein kinase homologue controls phosphorylation of ganciclovir in human cytomegalovirus-infected cells. *Nature* **358**: 162–164.
 103. Tam, A., et al. 2003. Murine cytomegalovirus with a transposon insertional mutation at open reading frame M35 is defective in growth in vivo. *J. Virol.* **77**:7746–7755.
 104. Tang, Q., and G. G. Maul. 2003. Mouse cytomegalovirus immediate-early protein 1 binds with host cell repressors to relieve suppressive effects on viral transcription and replication during lytic infection. *J. Virol.* **77**:1357–1367.
 105. Tang, Q., E. A. Murphy, and G. G. Maul. 2006. Experimental confirmation of global murine cytomegalovirus open reading frames by transcriptional detection and partial characterization of newly described gene products. *J. Virol.* **80**:6873–6882.
 106. Telford, E. A., M. S. Watson, K. McBride, and A. J. Davison. 1992. The DNA sequence of equine herpesvirus-1. *Virology* **189**:304–316.
 107. Thale, R., P. Lucin, K. Schneider, M. Eggers, and U. H. Koszinowski. 1994. Identification and expression of a murine cytomegalovirus early gene coding for an Fc receptor. *J. Virol.* **68**:7757–7765.
 108. Thale, R., et al. 1995. Identification of the mouse cytomegalovirus genomic region affecting major histocompatibility complex class I molecule transport. *J. Virol.* **69**:6098–6105.
 109. Upton, J. W., W. J. Kaiser, and E. S. Mocarski. 2008. Cytomegalovirus M45 cell death suppression requires receptor-interacting protein (RIP) homotypic interaction motif (RHIM)-dependent interaction with RIP1. *J. Biol. Chem.* **283**:16966–16970.
 110. Valchanova, R. S., M. Picard-Maureau, M. Budt, and W. Brune. 2006. Murine cytomegalovirus m142 and m143 are both required to block protein kinase R-mediated shutdown of protein synthesis. *J. Virol.* **80**:10181–10190.
 111. Wagner, M., S. Jonic, U. H. Koszinowski, and M. Messerle. 1999. System-

- atic excision of vector sequences from the BAC-cloned herpesvirus genome during virus reconstitution. *J. Virol.* **73**:7056–7060.
112. Wing, B. A., G. C. Lee, and E. S. Huang. 1996. The human cytomegalovirus UL94 open reading frame encodes a conserved herpesvirus capsid/tegument-associated virion protein that is expressed with true late kinetics. *J. Virol.* **70**:3339–3345.
 113. Winkler, M., S. A. Rice, and T. Stamminger. 1994. UL69 of human cytomegalovirus, an open reading frame with homology to ICP27 of herpes simplex virus, encodes a transactivator of gene expression. *J. Virol.* **68**:3943–3954.
 114. Worrad, D. M., and S. Caradonna. 1988. Identification of the coding sequence for herpes simplex virus uracil-DNA glycosylase. *J. Virol.* **62**:4774–4777.
 115. Wright, D. A., S. I. Staprans, and D. H. Spector. 1988. Four phosphoproteins with common amino termini are encoded by human cytomegalovirus AD169. *J. Virol.* **62**:331–340.
 116. Wu, C. A., M. E. Carlson, S. C. Henry, and J. D. Shanley. 1999. The murine cytomegalovirus M25 open reading frame encodes a component of the tegument. *Virology* **262**:265–276.
 117. Xiao, J., T. Tong, X. Zhan, E. Haghjoo, and F. Liu. 2000. In vitro and in vivo characterization of a murine cytomegalovirus with a transposon insertional mutation at open reading frame M43. *J. Virol.* **74**:9488–9497.
 118. Xu, J., et al. 1994. Identification, sequencing and expression of the glycoprotein L gene of murine cytomegalovirus. *J. Gen. Virol.* **75**(Pt. 11):3235–3240.
 119. Zhan, X., M. Lee, J. Xiao, and F. Liu. 2000. Construction and characterization of murine cytomegaloviruses that contain transposon insertions at open reading frames m09 and M83. *J. Virol.* **74**:7411–7421.
 120. Zhang, G., et al. 2007. Antisense transcription in the human cytomegalovirus transcriptome. *J. Virol.* **81**:11267–11281.
 121. Zhu, J., et al. 2003. In vitro and in vivo characterization of a murine cytomegalovirus with a mutation at open reading frame m166. *J. Virol.* **77**:2882–2891.
 122. Ziegler, H., W. Muranyi, H. G. Burgert, E. Kremmer, and U. H. Koszinowski. 2000. The luminal part of the murine cytomegalovirus glycoprotein gp40 catalyzes the retention of MHC class I molecules. *EMBO J.* **19**:870–881.
 123. Zimmermann, A., et al. 2005. A cytomegaloviral protein reveals a dual role for STAT2 in IFN-{gamma} signaling and antiviral responses. *J. Exp. Med.* **201**:1543–1553.